

Global Temperature Update Through 2013

21 January 2014

James Hansen, Makiko Sato and Reto Ruedy

Summary. Global surface temperature in 2013 was $+0.6^{\circ}\text{C}$ ($\sim 1.1^{\circ}\text{F}$) warmer than the 1951-1980 base period average, thus the seventh warmest year in the GISS analysis. The rate of global warming is slower in the past decade than in the prior three decades. Slower growth of net climate forcings and cooling in the tropical Pacific Ocean both contribute to the slower warming rate, with the latter probably the more important effect. The tropical Pacific cooling is probably unforced variability, at least in large part. The trend toward an increased frequency of extreme hot summer anomalies over land areas has continued despite the Pacific Ocean cooling. The “bell curves” for observed temperature anomalies show that, because of larger unforced variability in winter, it is more difficult in winter than in summer to recognize the effect of global warming on the occurrence of extreme warm or cold seasons. It appears that there is substantial likelihood of an El Niño beginning in 2014, and as a result a probable record global temperature in 2014 or 2015.

The update through 2013 of the GISS (Goddard Institute for Space Studies) global temperature analysis¹ (Fig. 1), available in detail on the GISS web site (<http://data.giss.nasa.gov/gistemp/>), reveals 2013 as slightly warmer than the preceding two years and nominally the 7th warmest year in the GISS analysis. Although there are several sources of error in the estimated temperature, the biggest error in comparing global temperature for nearby years is from the incomplete spatial coverage of data. Uncertainty between nearby years is a few hundredths of a degree Celsius¹. Thus, accounting for this uncertainty, we say that 2005 and 2010 tie for warmest year, 1998, 2002, 2003, 2006, 2007, 2009 and 2013 tie as the 3rd through 9th warmest, and 2012 is the 10th warmest. The 14 warmest years all occurred since 1998 (including 1998). Large year-to-year temperature fluctuations in Fig. 1 are caused mainly by natural oscillations of tropical Pacific sea surface temperatures as summarized by the Niño index (lower part of Fig. 1), which we illustrate with higher resolution in a later figure.

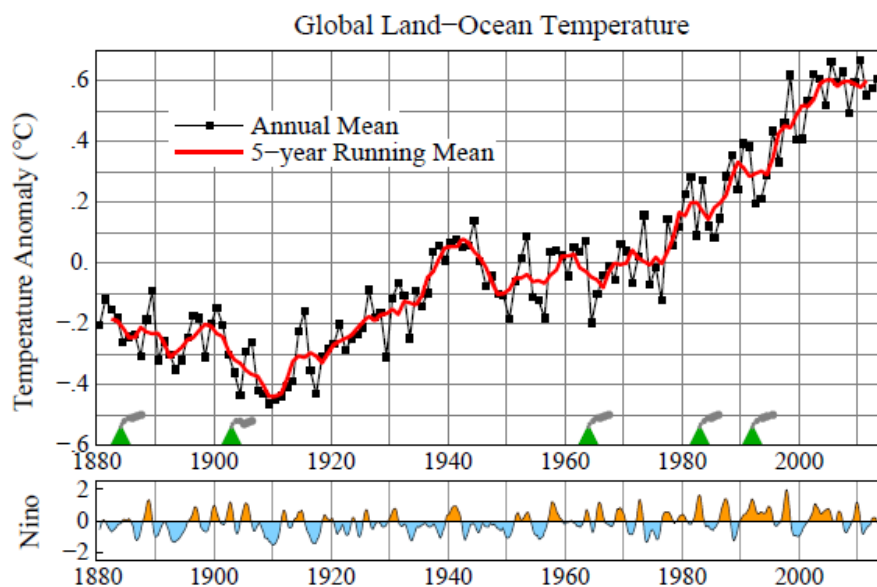


Fig. 1. Global surface temperatures relative to 1951-1980. The Niño index is based on sea surface temperature in the Niño 3.4 area (5N-5S, 120-170W) in the eastern tropical Pacific² for 1951-1980 base period. Green triangles mark times of volcanic eruptions that produced an extensive stratospheric aerosol layer.

2013 Mean Surface Temperature Anomaly (°C): 1951-80 Base Period

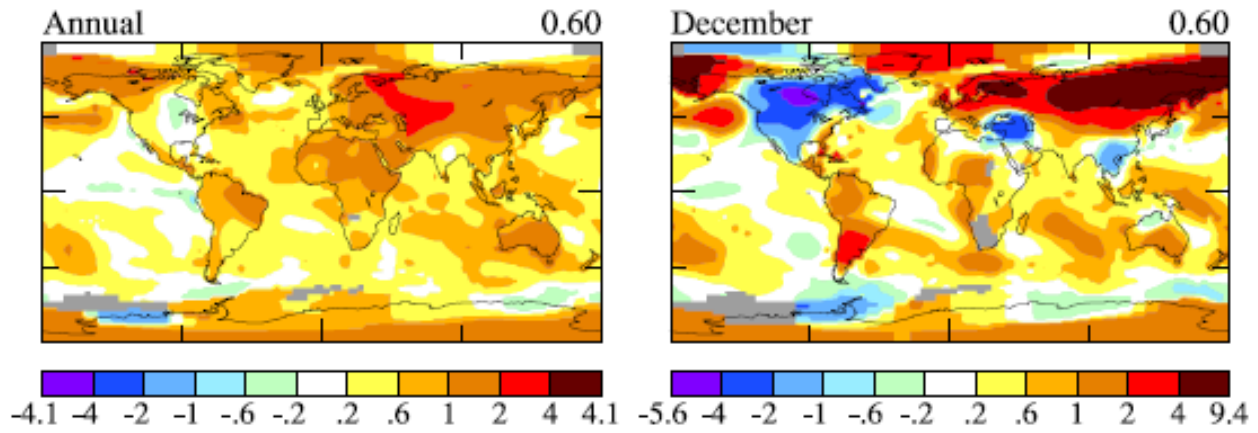


Fig. 2. Annual and December 2013 temperature anomalies relative to 1951-1980 base period.

Land areas were much warmer than the 1951-1980 base period almost everywhere (Fig. 2), the principal exceptions being the United States, Canada and India, which were close to the base period average. The final month of 2013 (Fig. 2, right side) was exceptionally cold in North America (as much as 5°C colder than the 1951-1980 climatology) and exceptionally warm in northeast Europe and Siberia (as much as 9°C warmer than climatology). Predictably, these weather patterns, which continued into early January, caused many in the North American media to question the reality of global warming, but in fact the December global temperature anomaly (+0.6°C) was the same as the annual mean anomaly.

A weak La Niña-like cooling of the equatorial Eastern Pacific Ocean was present most of the year, but weakened in Northern Hemisphere Autumn (Fig. 3). The weakening of that pattern contributed to 2013 having the second warmest Sep-Oct-Nov in the 134-year record. Regional seasonal-mean temperature variability is commonly as large as 1-2°C, which compares with global warming of about 0.6°C since the 1951-1980 base period. Thus it is not surprising when a season, such as the 2013 North American Spring, is cooler than the 1951-1980 climatology (Fig. 3). Below we will illustrate how the frequency distribution of seasonal temperature anomalies (the “bell curve”) has changed in recent years.

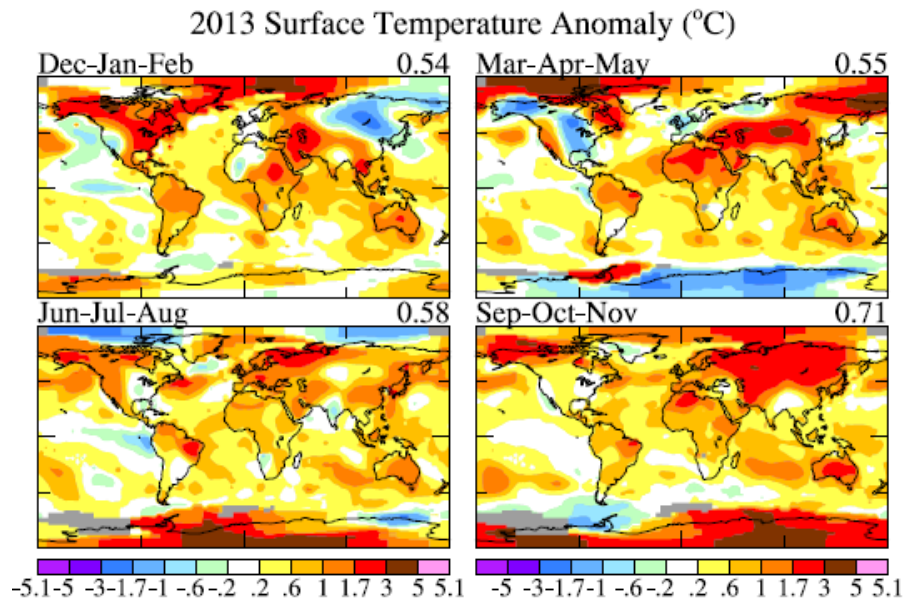


Fig. 3. Seasonal-mean temperature anomalies. Dec-Jan-Feb map employs December 2012 data.

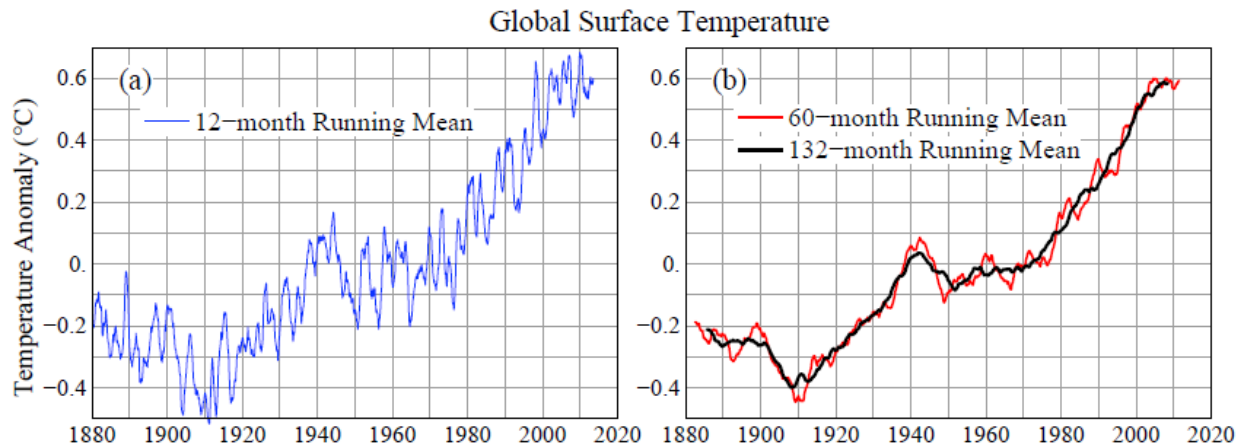


Fig. 4. Global surface temperature relative to 1951-1980 mean for (a) 12-month running mean, and (b) 5-year and 11-year running means.

Although Fig. 1 might leave an impression that global warming stopped after 1998, closer examination, including Fig. 4, shows that warming has only slowed in the past decade. The 12-month running-mean (Fig. 4a) is helpful in comparing global temperature peaks and valleys associated with successive El Niños and La Niñas, as these phenomena do not generally coincide with the calendar year. Recent successive La Niñas (e.g., 1999, 2008, 2011) are each warmer, and successive El Niños show slight warming even though 1998 had the strongest El Niño. The century time-scale warming trend, including continual warming since the mid-1970s, has been conclusively associated with the predominant global climate forcing^a, human-made greenhouse gases³, which began to grow substantially early in the 20th century. The approximate stand-still of global temperature during 1940-1975 is generally attributed to an approximate balance of aerosol cooling and greenhouse gas warming during a period of rapid growth of fossil fuel use with little control on particulate air pollution, but satisfactory quantitative interpretation has been impossible because of the absence of adequate aerosol measurements⁴.

The five-year running-mean of the global temperature (Fig. 4b) has been flat for several years, but the 11-year mean continues to rise at a reduced rate. Below we discuss the possible roles of climate forcings and unforced climate variability in this slowdown of global warming.

For the past several decades each successive decade has been notably warmer than the preceding decade (Fig. 5). The first three years of the present decade (lower right of Fig. 5) have about the same average temperature as the preceding decadal mean. However, we can predict with reasonably high confidence that the present decade as a whole will be warmer than the preceding decade. The principal basis for that expectation is knowledge that the planet is out of energy balance⁵, more energy coming in than going out, which is a consequence mainly of increasing greenhouse gases over the past century^{3,5}, as well as knowledge that greenhouse gases are continuing to increase. It is conceivable, though unlikely, that negative climate forcing, e.g., from large volcanic eruptions, could alter the planet's energy balance enough to keep the current decade slightly cooler than the prior decade.

Close examination of Fig. 3 shows that most land areas are warmer in the past three years than in the prior decade, but the Eastern Pacific Ocean is cooler. Kosaka and Xie⁶ have compared global climate simulations with and without a constraint of specified observed sea surface temperatures in the tropical eastern Pacific Ocean, concluding that the observed Pacific cooling largely accounts for the “hiatus” in global warming during the past 15 years. Their experiments, however, do not identify the cause of the Eastern Pacific cooling, which could include effects of climate forcings as well as unforced variability.

^a A climate forcing is an imposed perturbation of the planet's energy balance that tends to alter global temperature.

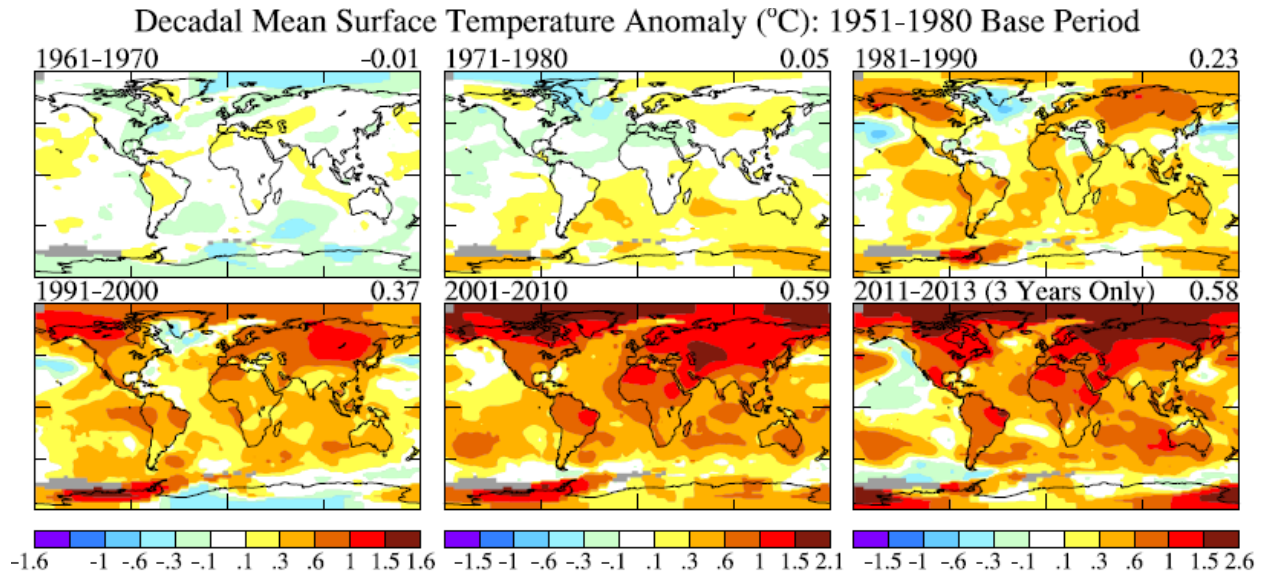


Fig. 5. Decadal surface temperature anomalies relative to 1951-1980 base period. The current decade (lower right) has three years of data.

Seasonal and geographical dependence of observed temperature change support the Kosaka and Xie interpretation that the Eastern Pacific Ocean temperature is the principal drive for the reduced global warming rate. Specifically, as shown in Fig. 6, there has been no slowdown in the warming in the summer season (Jun-Jul-Aug in the Northern Hemisphere, Dec-Jan-Feb in the Southern Hemisphere) over land in either hemisphere. Continents largely respond locally to the increasing greenhouse forcing in the summer as the dynamical exchange of heat with the ocean is reduced in summer.

In contrast, winter temperature over land has declined in the past 10 years (Fig. 6a). There has been recent speculation that observed loss of Arctic sea ice may spur winter cold air outbreaks. On the other hand, Fig. 6a shows that there have been large oscillations in winter land temperature in the past when large Arctic sea ice reductions are not known to have occurred and seem unlikely, although accurate sea ice data are not available for those earlier times. Kosaka and Xie simulations suggest that the recent winter cooling is more a consequence of tropical ocean temperatures. Climate models yield larger long-term warming in winter than in summer, even when considering only land areas. Thus the recent downturn of winter temperature over Northern Hemisphere land is unlikely to continue.

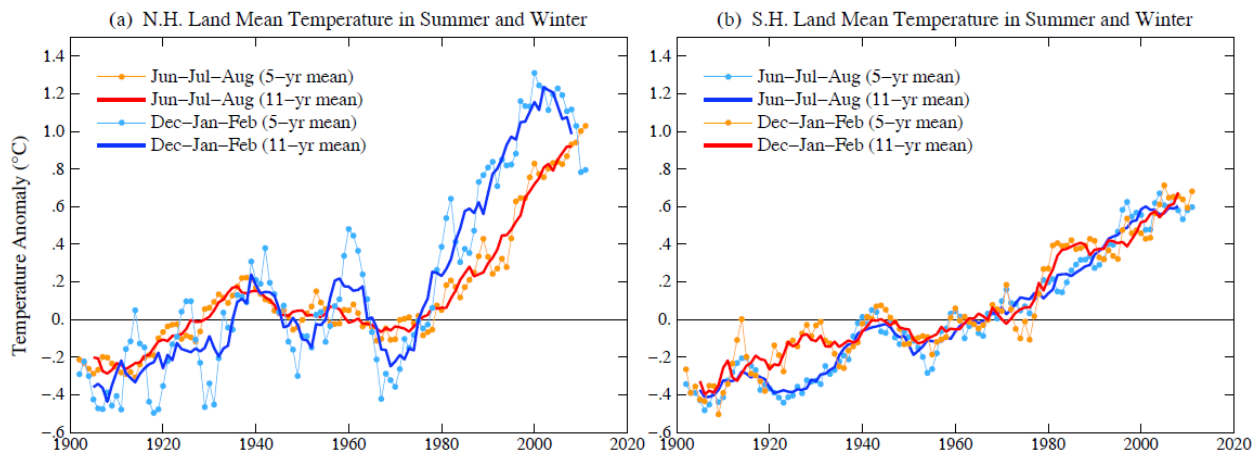


Fig.6. Summer and winter temperature anomaly over land in the Northern (a) and Southern Hemispheres (Southern Hemisphere land excludes Antarctica).

Surface Temperature Anomaly (°C): Base Period = 1951-1980

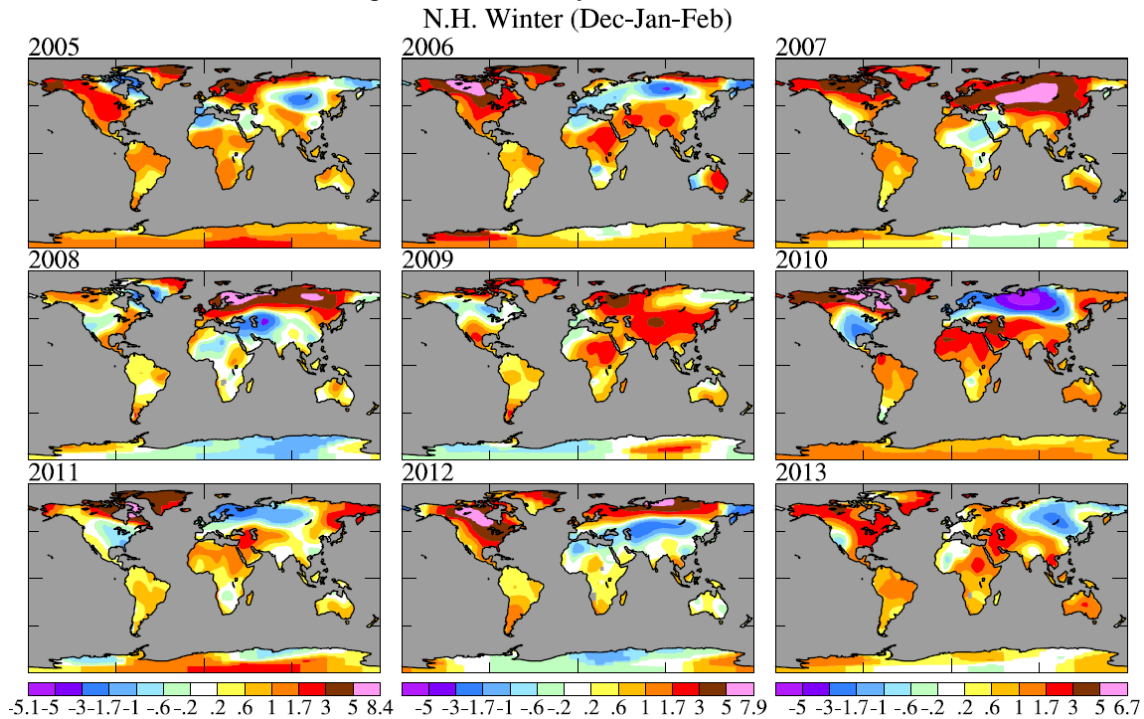


Fig. 7. Surface temperature anomalies relative to 1951-1980 in each of the past nine years during Northern Hemisphere winter (Dec-Jan-Feb).

Temperature Variability. The interannual variability of local or regional temperature over land areas in middle and high latitudes is much larger in winter than in summer. High winter variability is related to the large temperature gradient between tropical and polar latitudes in winter. Local temperature in winter is thus highly dependent on the wind direction, which varies as the weather patterns change. The standard deviation^b of seasonal mean local temperature is typically 3-4 times larger in the winter than in the summer at middle and high latitude continental regions in the Northern Hemisphere⁷.

Because of the large interannual variability of regional winter temperature, it is common to have large areas of land in any given winter that are colder than the 1951-1980 average climate, as shown in Fig. 7 for the past nine Northern Hemisphere winters. In contrast, because of the smaller variability in the summer, the warming of the past several decades has reached a level exceeding that variability, and thus almost all areas are warmer than the 1951-1980 climatology (Fig. 8). Stated differently, in a given region almost all summers are now warmer than the average summer during 1951-1980. Therefore it is not surprising that the public may find it easier to agree that the climate is becoming warmer during summer. In contrast, in middle and high latitudes there is a substantial likelihood that any given winter will be unusually cold, even in comparison with the average climate half a century ago.

This “substantial likelihood” is made quantitative via observed “bell curves” for the frequency of occurrence of seasonal mean temperature anomalies (Fig. 9). The frequency of occurrence of a given temperature anomaly approximates well a Gaussian bell curve during the 1951-1980 climatology period, with the anomalies measured in units of the local standard deviation of seasonal-mean temperature, a normalization that divides out the larger winter variability. (The increase of extreme hot anomalies in the 21st century is slightly exaggerated by the decreasing number of measurement stations in recent years⁸.)

^b The standard deviation is a measure of typical variability about the average. About two-thirds of the cases fall within 1 standard deviation of the average and about 95 percent fall within 2 standard deviations.

Surface Temperature Anomaly (°C): Base Period = 1951-1980

N.H. Summer (Jun-Jul-Aug)

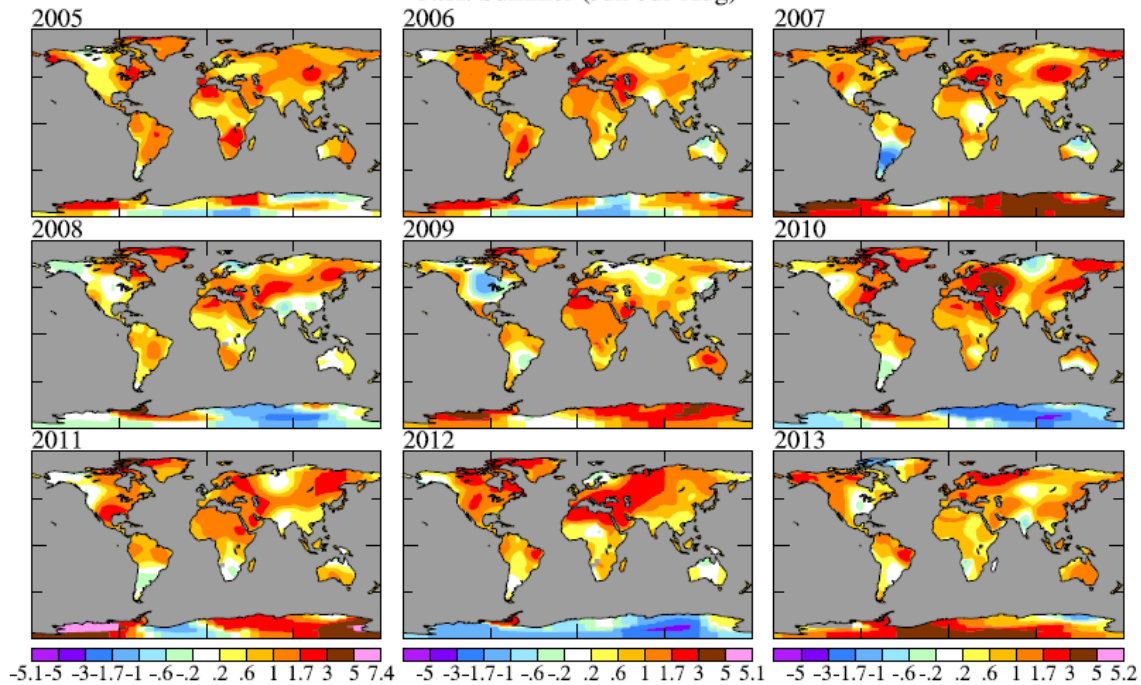


Fig. 8. Same as Fig. 7, but for Northern Hemisphere summer (Jun-Jul-Aug).

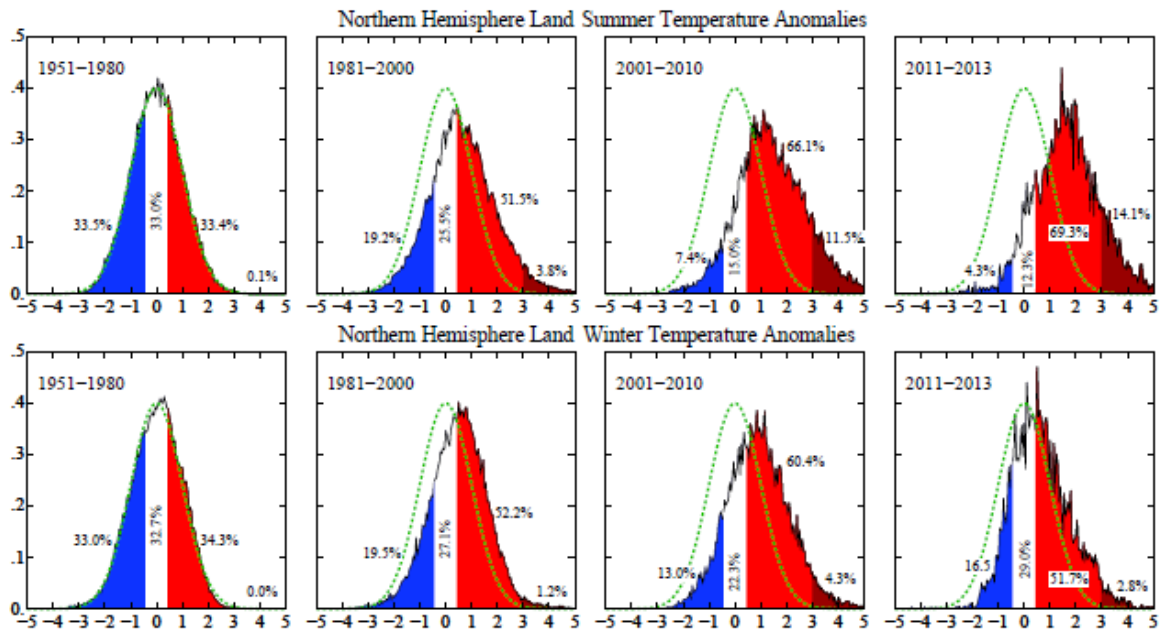


Fig. 9. Frequency of occurrence of local Jun-Jul-Aug (top row) and Dec-Jan-Feb (bottom) temperature anomalies for Northern Hemisphere land areas in units of the local standard deviation (horizontal axis).

The “climate dice” became noticeably “loaded” by the first decade of the 21st century, as shown by the third column in Fig. 9. The chance of having a summer-mean temperature anomaly warmer than +3 standard deviations relative to 1951-1980 climate now exceeds 10%. However, the observed bell curve for winter remains closer to the idealized (Gaussian) 1951-1980 bell curve. The likelihood of having a winter judged unusually cold by 1951-1980 standards (blue area in Fig. 9) remains large enough to correspond to approximately one face of a 6-sided die and increased somewhat in the past three years.

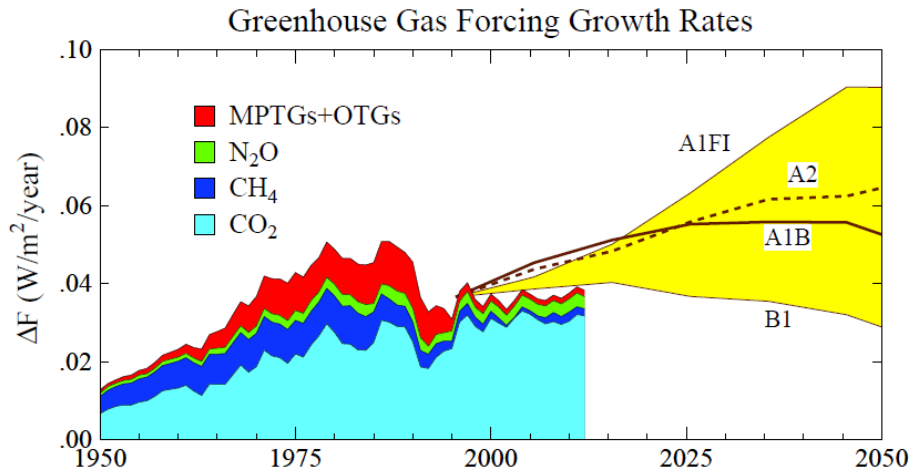


Fig. 10. Update⁹ of 5-year mean of the growth rate of climate forcing by well-mixed greenhouse gases; ozone and stratospheric water vapor, neither well-mixed nor well-measured, are not included.

Climate Forcings. Slowdown of global warming can be largely accounted for by relative cooling in the Pacific Ocean (lower row, Fig. 5), but changes of climate forcings may play a role. The largest climate forcing is from increasing greenhouse gases (GHGs), principally CO₂ (Fig. 10). The annual increment of GHG forcing peaked at ~ 0.05 W/m² in the 1980s, then declined to ~ 0.035 W/m² by 1990 (Fig. 10)^{9,10}. The decline was due to phase-out of ozone-depleting gases and reduced growth of CH₄.

The airborne fraction of fossil fuel CO₂ emissions has declined¹¹ and forcing per CO₂ increment decreases as CO₂ increases due to partial saturation of absorption bands. Thus the CO₂ forcing growth rate has slowed. The atmospheric CO₂ growth rate continues to increase (Fig. 11) due to rapid growth of fossil fuel emissions. CO₂ change correlates with global temperature change (Fig. 11), the maximum correlation (56%) occurring, as expected, with CO₂ change lagging temperature change (by 10 months).

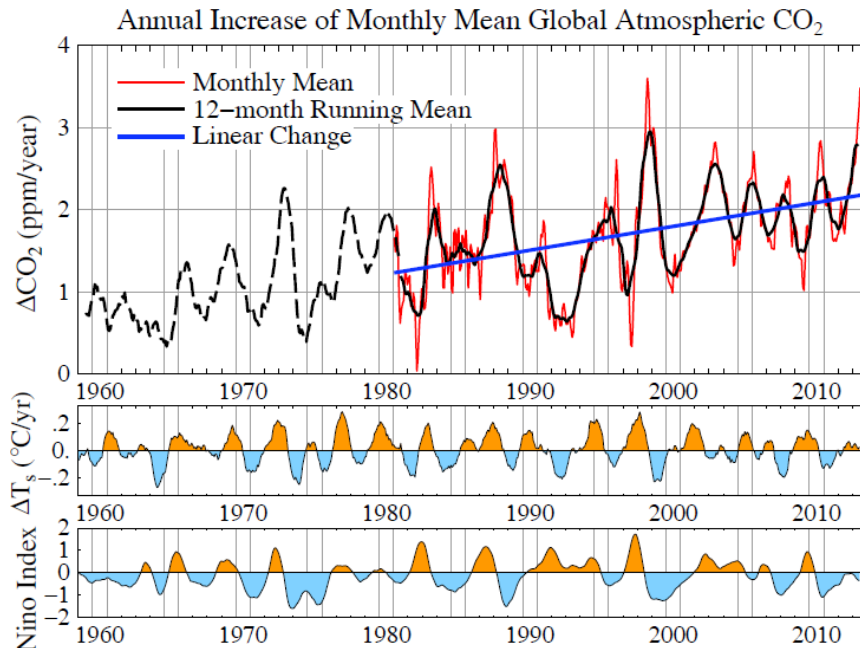


Fig. 11. Annual increase of CO₂ based on data from the NOAA Earth System Research Laboratory¹²; prior to 1981 the CO₂ change is based on only Mauna Loa, Hawaii. Temperature changes are 12-month running means for the globe and Niño 3.4 area¹; Niño index uses NOAA's 1981-2010 base period.

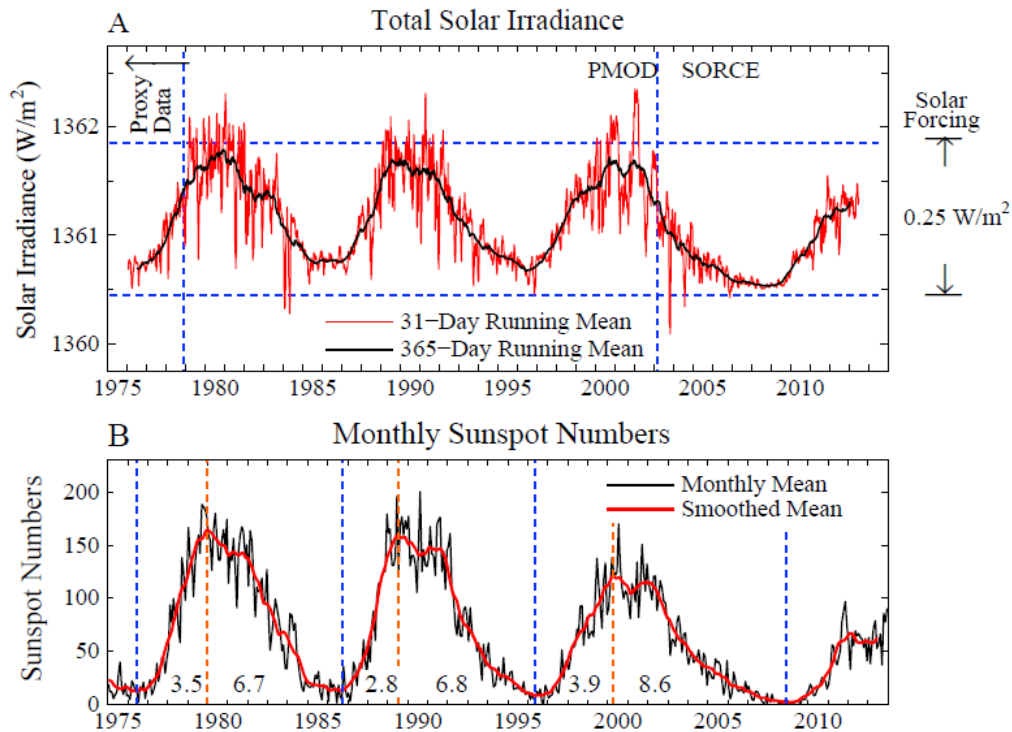


Fig. 12. Update¹³ of solar irradiance from composite of several satellite-measured time series. Data through 28 February 2003 are from Frohlich and Lean^{14,15}. Subsequent data are from [University of Colorado Solar Radiation & Climate Experiment](http://www.colorado.edu/~solar/) normalized to match means over the final 12 months of the Frohlich and Lean data. Sunspot data from <http://sidc.oma.be/sunspot-data/>

Solar irradiance variation is often assumed to be a main driver of climate change. Solar irradiance has been measured from satellites since the late 1970s. The left scale in Fig. 12(a) is the energy passing through an area perpendicular to the Sun-Earth line. Absorbed solar energy averaged over Earth's surface is $\sim 240 \text{ W/m}^2$, so the full amplitude of the variability of solar climate forcing is $\sim 0.25 \text{ W/m}^2$. Monthly sunspot numbers (Fig. 12b) support the conclusion that the solar irradiance in the current solar cycle is significantly lower than in the three preceding solar cycles. Amplification of the direct solar forcing is conceivable, e.g., through effects on ozone or atmospheric condensation nuclei, but empirical data place a factor of two upper limit on the amplification, with the most likely forcing in the range 100-120% of the directly measured solar irradiance change⁵.

Solar irradiance may have been reduced over the past decade by as much as half the full amplitude of measured irradiance variability (Fig. 12), yielding a negative forcing of, say, -0.12 W/m^2 . This compares with a decadal increase of GHG forcing about three times larger. However, we should (1) compare the solar forcing with the net of other forcings not the GHG forcing alone, which enhances the importance of solar change, because the net forcing is smaller than the GHG forcing, and (2) consider forcing changes on longer time scales, which diminishes the importance of solar change, because solar variability is mainly oscillatory while the GHG forcing increases monotonically. We conclude that solar forcing is not negligible and contributed modestly to the global warming slowdown in the past decade, but its effect was small¹⁶ and overwhelmed by long-term growth of GHGs, as confirmed by the fact that Earth was out of energy balance, more energy coming in than going out, even during the deep 2005-2010 solar minimum⁵.

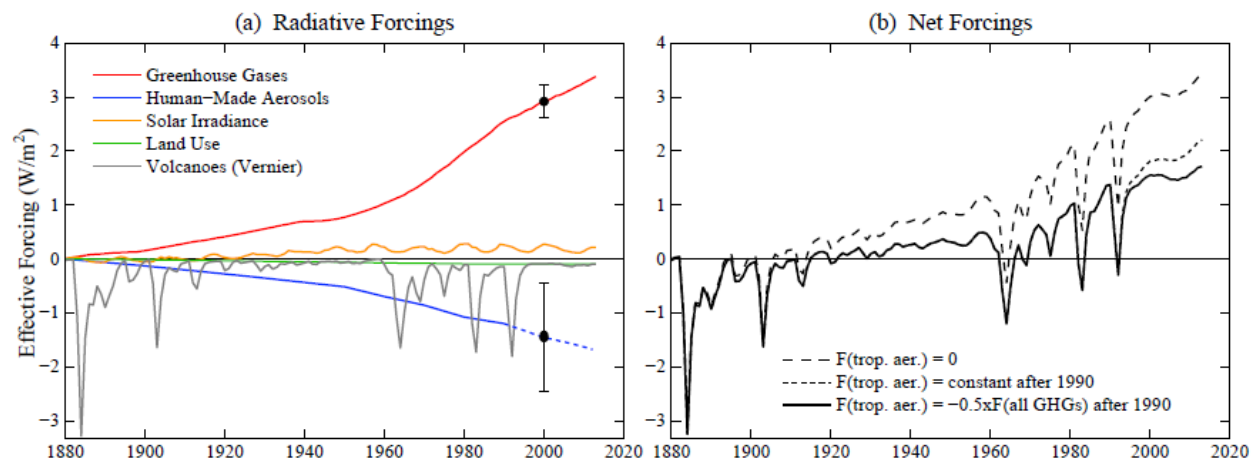


Fig. 13. Estimated climate forcings. Uncertainties are small for well-mixed GHGs but large for unmeasured tropospheric aerosols. Aerosol forcing includes indirect effects on clouds and snow albedo. GHGs include O_3 and stratospheric H_2O , in addition to well-mixed GHGs.

Unfortunately, other important forcings are not measured. Atmospheric aerosols^c surely cause the 2nd largest human-made forcing, but its value is very uncertain^{3,4}. Fig. 13 includes aerosol forcing estimated by Hansen et al.¹⁷ up to 1990^d. For the later aerosol forcing we show two assumptions: (1) constant 1990 tropospheric aerosol forcing, and (2) aerosol forcing half of the GHG forcing, but opposite in sign. The first assumption would be good if reduction of aerosol forcing from developed countries was sufficient to offset the effect of increased aerosols from developing countries. The arithmetic of this comparison is not simple, because the aerosol climate forcing is not simply related to aerosol mass or number. For example, the “indirect” forcing, i.e., the change of cloud properties due to aerosol change, is highly non-linear in aerosol amount. Thus aerosol forcing due to aerosol increase in the relatively less polluted atmosphere over the Pacific Ocean is not balanced by an equal reduction of aerosols in polluted continental air.

The truth may fall between those two assumptions, but that conclusion is only an educated guess. An empirical assessment of aerosol forcing -1.6 W/m^2 for 2005-2010, based mainly on Earth’s observed energy imbalance, favors the increasingly negative forcing (solid curve in Fig 13b). Qualitative support for increasing aerosol forcing is the fact that the largest change of fossil fuel emissions was increased coal burning in the Far East, an aerosol source that probably would increase aerosol forcing over the Pacific Ocean. However, such circuitous inferences about the aerosol forcing are highly unsatisfactory.

The tragedy about the unknown aerosol climate forcing is that the first satellite mission capable of measuring global aerosol and cloud microphysical properties with the accuracy needed to assess changes of aerosol climate forcing⁴ should have been in place for a few years now, but because of a launch failure it ended up in the Antarctic Ocean instead of in space. As yet there are no plans to replace that mission. Although many satellite instruments can detect aerosols and estimate limited aerosol properties, accurate measurement of the ~ 10 aerosol parameters needed to assess climate forcing requires multi-spectral polarization observations to an accuracy of the order of 0.1% at wavelengths from the near-ultraviolet to the near-infrared at a wide range of scattering angles⁴. In the absence of such data continued over a number of years, the aerosol climate forcing and its changes in time will remain highly speculative.

^c Aerosols are fine particles in the air. Visible air pollution is composed especially of sulfates arising from sulfur in fossil fuels and black soot and organic carbon from incomplete combustion of fossil fuels and biofuels.

^d One change is made to climate forcings: stratospheric aerosol optical depth for 1991-2012 is from a new analysis kindly provided by Jean-Paul Vernier of NASA LaRC. The principal change is a reduction of optical depth after the 1991 Pinatubo eruption in the lowest part of the stratosphere where satellite measurements were saturated.

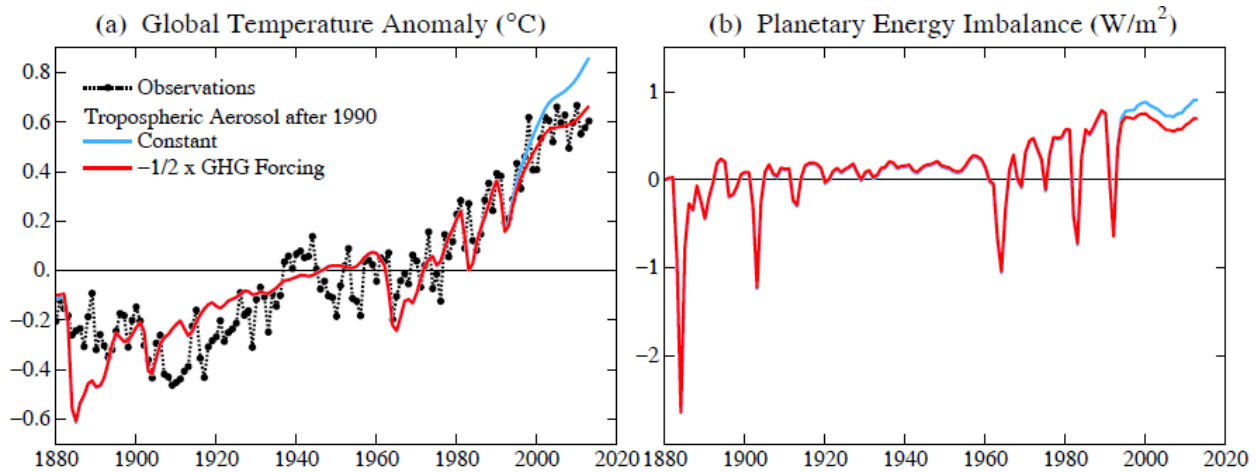


Fig. 14. Calculated global temperature anomaly and planetary energy imbalance using a simple climate response function.^{18,5} Calculations use the intermediate climate response function (Fig. 5 in reference 5) with the climate forcing using two alternatives for aerosols after 1990 (our present Fig. 13).

If the assumption that aerosol forcing increased (became more negative) in the past decade is correct, then the net climate forcing has been quite flat during the past 15-20 years (Fig. 13b). If aerosol forcing is taken as unchanging since 1990, the growth rate of the net climate forcing has been slower in the past 15-20 years than it was in the preceding three decades, but only slightly. Thus a slowdown in growth of the net climate forcing probably contributed to the slowdown of the global warming rate, but was it a slight contribution or a substantial one? We can investigate the impact of these alternative forcing histories quantitatively via some simple computations with a (Green's function) climate response function.

The climate response function we employ⁵ is appropriate for an equilibrium global climate sensitivity 3°C for $2\times\text{CO}_2$, which is consistent with the climate sensitivity implied by Earth's paleoclimate history¹⁹. Results of the computations with this response function, carried out as in our prior energy imbalance paper⁵, are shown in Fig. 14. The results depend substantially on the assumed aerosol scenario in the past two decades. If the aerosol forcing continued to increase, which we suggest is likely given the increased coal burning in the Far East, then a slowdown in warming comparable to that observed is expected.

Earth's measured energy imbalance provides a valuable check on this interpretation (Fig. 14b). The calculated energy imbalance with increasing aerosols is $\sim+0.6 \text{ W/m}^2$, but $\sim+0.8 \text{ W/m}^2$ if aerosol forcing remained constant after 1990. The observed energy imbalance⁵ is about $+0.6 \text{ W/m}^2$, composed of $\sim+0.4 \text{ W/m}^2$ heat gain by the upper 1500 m of the ocean, $\sim+0.1 \text{ W/m}^2$ heat gain by the deeper ocean, and $\sim+0.1 \text{ W/m}^2$ as the sum of all other terms including melting of ice and heat storage in the ground, lakes, and air.

These results emphasize the importance of making the high precision measurements of aerosol and cloud microphysics that are needed to infer the changing aerosol climate forcing. Thus it is puzzling that no reflight has been scheduled for the mission⁴ that is capable of making such measurements.

We conclude that a slowdown of the growth rate of the net climate forcing probably contributed to the slowdown of global warming in the past 15 years. The slower increase of climate forcing cannot by itself account for a long global temperature standstill, because we know that the planet continued to be well out of energy balance, more energy coming in from the sun than energy radiated to space. The dynamic variability of tropical Pacific sea surface temperature, i.e., the ENSO (El Niño Southern Oscillation),² can play a significant role on temperature change over a decade and it has a dominant role in interannual fluctuations. Thus, for the sake of discussing recent temperature change and expectations for continuing global temperature change, we need to examine the recent and current status of the ENSO.

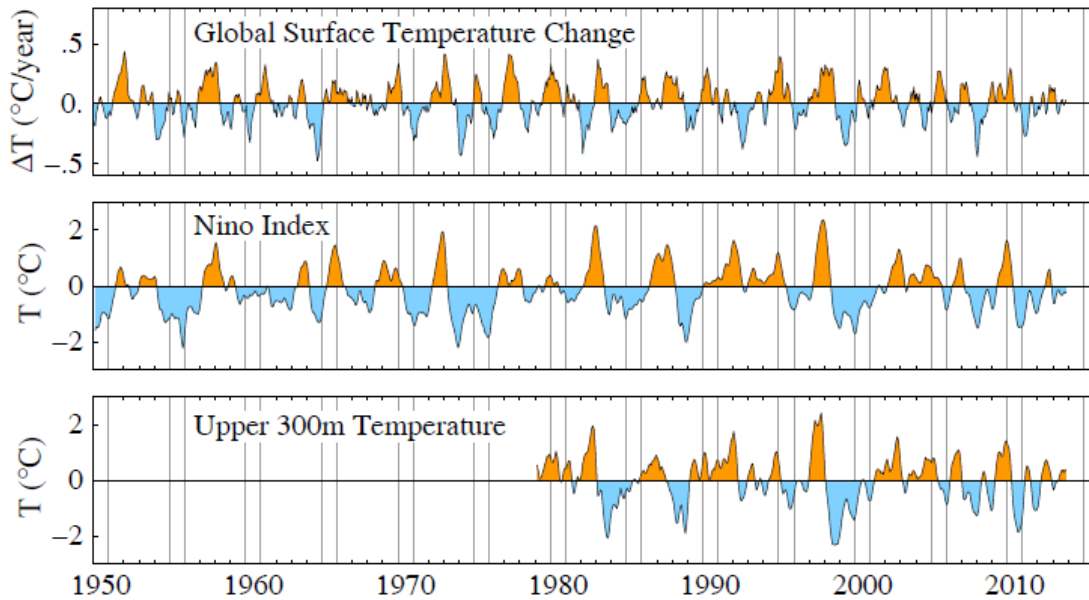


Fig. 15. Three-month-running-means of global surface temperature change, Niño3.4 index, and the temperature of the upper 300 m of the equatorial Pacific Ocean (100W-180W).

Near-Term Climate Change Expectations. The tropical Pacific is presently in the ENSO-neutral state, with both the equatorial sea surface temperatures and heat content of the upper 300 m of the ocean near the average of the past several decades (Fig. 15). The trend of the Niño3.4 index (middle curve in Fig. 15) over the past decade was toward cooler temperature, which, as Kosaka and Xie⁶ have shown quantitatively, can account for the lack of a global warming trend during the past decade despite the small warming trend that would be expected as a result of climate forcings alone (14a).

What should we expect for near-term global temperature change, given what we know about climate forcings and the state of the tropical Pacific Ocean? The latter is the critical factor, because of the known large impact of tropical Pacific Ocean surface temperature on interannual global temperature change.

First a few background comments may be warranted. In the La Niña phase or the ENSO-neutral state of the El Niño Southern Oscillation, east-to-west trade winds are pushing warm equatorial surface water to the west, so the warmest SSTs (sea surface temperatures) are located in the Western Equatorial Pacific near Indonesia. In this normal ENSO state, cold deep water upwells near the South American coast, thus maintaining a strong east-west temperature gradient. Associated with this tropical SST gradient is a longitudinal circulation pattern in the atmosphere, the Walker cell, with rising air and heavy rainfall in the Western Equatorial Pacific and sinking air and drier conditions in the Eastern Equatorial Pacific.

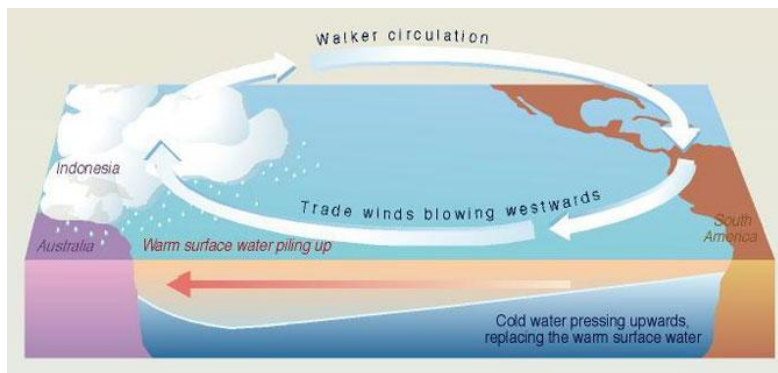


Fig. 16. Cartoon diagram of Walker circulation.²⁰

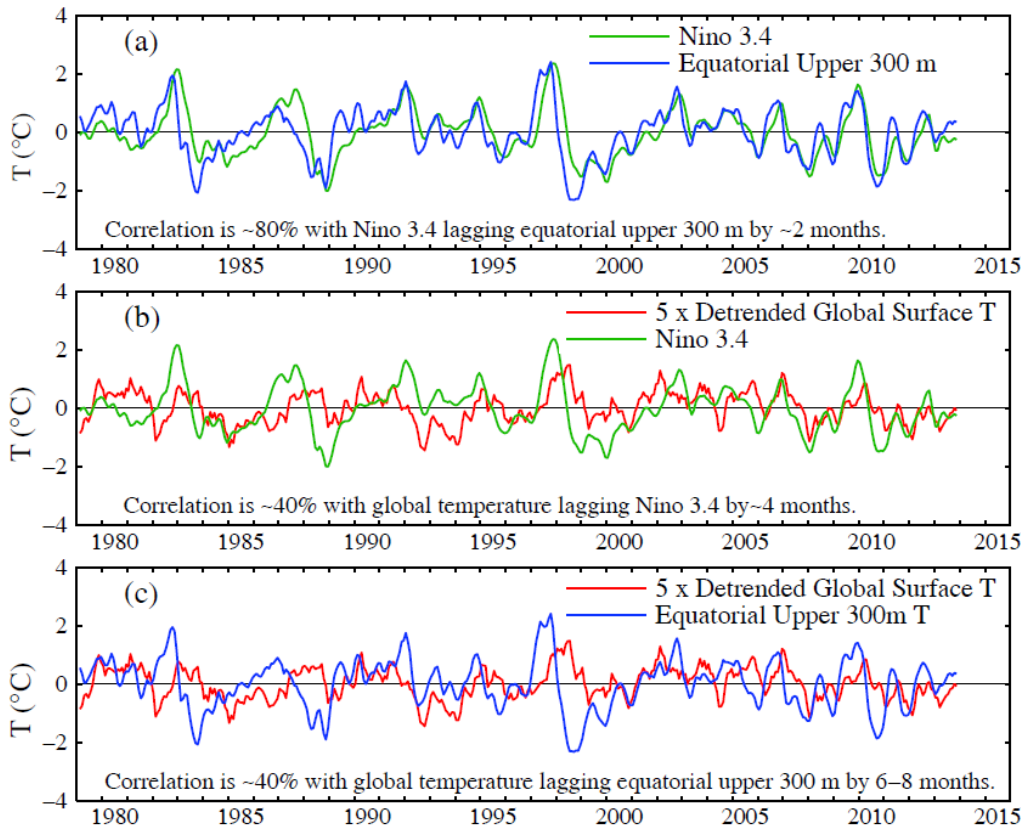


Fig. 17. Comparison and correlations of the three quantities shown in Fig. 15.

The easterly surface winds enhance upwelling of cold water in the East Pacific, causing a powerful (Bjerknes) positive feedback, which tends to maintain the normal ENSO state, as the SST gradient and resulting higher pressure in the Eastern Equatorial Pacific support the east-to-west trade winds. The normal state is occasionally upset when, by chance, the east-to-west trade winds slacken, allowing warm water piled up in the west to slosh back toward South America. If the fluctuation is large enough, the Walker circulation breaks down and the Bjerknes feedback loses power, the east-to-west winds weaken, and warm waters move more strongly toward South America, cutting off or diminishing the upwelling of cold water along the South American coast. In this way a classical El Niño is born.

Correlations of global temperature, the Niño3.4 index, and the heat content of the upper 300 meters of the equatorial Pacific ocean reveal that the upper ocean heat content leads the Niño3.4 index on average by 2 months, and the Niño3.4 index in turn leads global temperature by another 4 months on average. In the case of the two unusually strong El Niños of the past half century (1982-3 and 1997-8) the lag of global temperature is a few months longer.

So what are the near-term prospects? El Niño depends on fickle wind anomalies for initiation, so predictions are inherently difficult, but conditions are ripe for El Niño initiation in 2014. About half of the climate models catalogued by the International Research Institute predict that the next El Niño will begin by summer 2014, with the other half predicting ENSO neutral conditions²¹. The mean NCEP forecast²¹ issued 13 January has an El Niño beginning in the summer of 2014, although a significant minority of the ensemble members predicts ENSO neutral conditions for 2014.

The strength of an El Niño, too, depends on the fickle wind anomalies at the time of initiation. We speculated²² that the likelihood of “super El Niños, such as those in 1982-3 and 1997-8, has increased. Our rationale was that global warming increased SSTs in the Western Pacific, without yet having much

effect on the temperature of upwelling deep water in the Eastern Pacific (Fig. 2 above), thus allowing the possibility of a larger swing of Eastern Pacific temperature. Recent paleoclimate²³ and modeling²⁴ studies find evidence for an increased frequency of extreme El Niños with global warming.

Assuming that an El Niño begins in summer 2014, 2014 is likely to be warmer than 2013 and perhaps the warmest year in the instrumental record. However, given the lag between El Niño initiation and global temperature, 2015 is likely to have a temperature even higher than in 2014.

Summary. The recent slowdown of global warming is a consequence of both a slowdown in the growth rate of climate forcings and recent ENSO history. Given that the tropical Pacific seems to be moving toward the next El Niño, record global temperature is likely in the near term. However, the rate of future warming will depend upon changes of the tropospheric aerosol forcing, which is highly uncertain and unmeasured.

Acknowledgments. We thank Gavin Schmidt for comments on the draft manuscript.

Table 1. Rankings of annual global temperature in the GISS analysis.

2010	0.67 (0.668)	Tie 1-2
2005	0.66 (0.662)	Tie 1-2
2007	0.63 (0.629)	Tie 3-9
2002	0.62 (0.621)	Tie 3-9
1998	0.62 (0.620)	Tie 3-9
2003	0.61 (0.607)	Tie 3-9
2013	0.60 (0.604)	Tie 3-9
2009	0.60 (0.598)	Tie 3-9
2006	0.60 (0.598)	Tie 3-9
2012	0.58 (0.577)	10

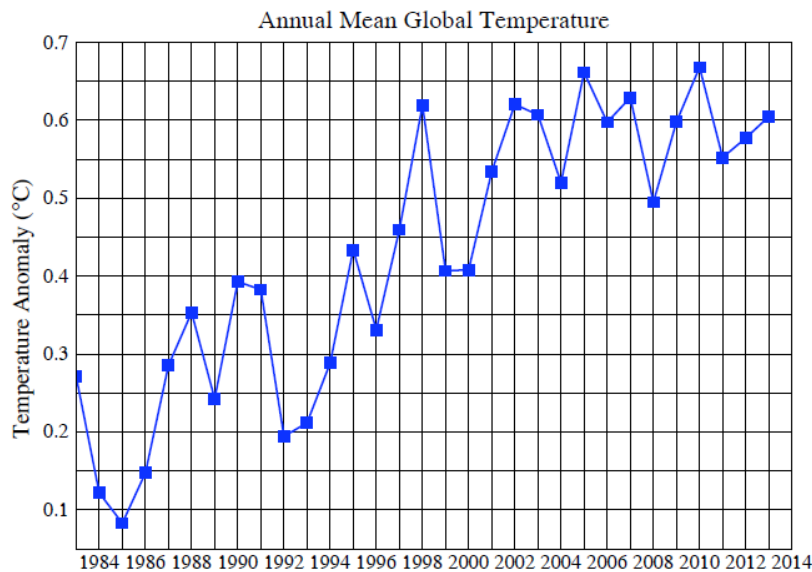


Fig. 18. Expanded recent temperatures to clarify year-to-year changes and slowdown of warming trend.

References

- ¹ Hansen, J., R. Ruedy, M. Sato, and K. Lo, 2010: [Global surface temperature change](#). *Rev. Geophys.*, **48**, RG4004, doi:10.1029/2010RG000345.
- ² Philander, S.G., *Our Affair with El Niño: How We Transformed an Enchanting Peruvian Current into a Global Climate Hazard*, Princeton Univ. Press, Princeton, NJ, 288 pp., 2006.
- ³ Intergovernmental Panel on Climate Change, *Climate Change 2007: The Physical Science Basis*, eds. S. Solomon, et al., Cambridge Univ. Press, New York, 2007.
- ⁴ Mishchenko, M.I., B. Cairns, G. Kopp, C.F. Schueler, B.A. Fafaul, J.E. Hansen, R.J. Hooker, T. Itchkawich, H.B. Maring, and L.D. Travis, 2007: [Accurate monitoring of terrestrial aerosols and total solar irradiance: Introducing the Glory mission](#). *Bull. Amer. Meteorol. Soc.*, **88**, 677-691, doi:10.1175/BAMS-88-5-677.
- ⁵ Hansen, J., M. Sato, P. Kharecha, and K. von Schuckmann, 2011: [Earth's energy imbalance and implications](#). *Atmos. Chem. Phys.*, **11**, 13421-13449, doi:10.5194/acp-11-13421-2011.
- ⁶ Kosaka, Y., Xie, S.P., Recent global warming hiatus tied to equatorial Pacific surface cooling, *Nature* **501**, 403-407, 2013, doi:10.1038/nature12534
- ⁷ Hansen, J., M. Sato, and R. Ruedy, 2012: [Perception of climate change](#). *Proc. Natl. Acad. Sci.*, **109**, 14726-14727, E2415-E2423, doi:10.1073/pnas.1205276109.
- ⁸ Hansen, J., M. Sato, and R. Ruedy, 2013: [Reply to Rhines and Huybers: Changes in the frequency of extreme summer heat](#). *Proc. Natl. Acad. Sci.*, **110**, E547-E548, doi:10.1073/pnas.1220916110.
- ⁹ Hansen, J., and M. Sato, 2004: [Greenhouse gas growth rates](#). *Proc. Natl. Acad. Sci.*, **101**, 16109-16114, doi:10.1073/pnas.0406982101.
- ¹⁰ Hansen, J., M. Sato, R. Ruedy, A. Lacis, and V. Oinas, 2000: [Global warming in the twenty-first century: An alternative scenario](#). *Proc. Natl. Acad. Sci.*, **97**, 9875-9880, doi:10.1073/pnas.170278997.
- ¹¹ Hansen, J., P. Kharecha, and M. Sato, 2013: [Climate forcing growth rates: Doubling down on our Faustian bargain](#). *Environ. Res. Lett.*, **8**, 011006, doi:10.1088/1748-9326/8/1/011006.
- ¹² Earth System Research Laboratory (2013) www.esrl.noaa.gov/gmd/ccgg/trends/
- ¹³ Hansen, J., P. Kharecha, M. Sato, V. Masson-Delmotte, F. Ackerman, D. Beerling, P.J. Hearty, O. Hoegh-Guldberg, S.-L. Hsu, C. Parmesan, J. Rockstrom, E.J. Rohling, J. Sachs, P. Smith, K. Steffen, L. Van Susteren, K. von Schuckmann, and J.C. Zachos, 2013: [Assessing "dangerous climate change": Required reduction of carbon emissions to protect young people, future generations and nature](#). *PLOS ONE*, **8**, e81648, doi:10.1371/journal.pone.0081648.
- ¹⁴ Frohlich C., J. Lean, 1998: The Sun's total irradiance: cycles and trends in the past two decades and associated climate change uncertainties. *Geophys. Res. Lett.* **25**, 4377-4380.
- ¹⁵ [Physikalisch Meteorologisches Observatorium Davos, World Radiation Center](#)
- ¹⁶ Meehl G.A., J.M. Arblaster, D.R. Marsh, 2013: Could a future "Grand Solar Minimum" like the Maunder Minimum stop global warming? *Geophys Res Lett* **40**, 1789-1793.
- ¹⁷ Hansen, J., M. Sato, R. Ruedy, P. Kharecha, A. Lacis, R.L. Miller, L. Nazarenko, K. Lo, G.A. Schmidt, G. Russell, I. et al., 2007: [Dangerous human-made interference with climate: A GISS modelE study](#). *Atmos. Chem. Phys.*, **7**, 2287-2312, doi:10.5194/acp-7-2287-2007.
- ¹⁸ Hansen, J., 2008: Climate threat to the planet: implications for energy policy and intergenerational justice, Bjerknæs lecture, American Geophysical Union, San Francisco, 17 December, available at: www.columbia.edu/~jeh1/presentations.shtml, 2008.
- ¹⁹ Hansen, J., M. Sato, G. Russell, and P. Kharecha, 2013: [Climate sensitivity, sea level, and atmospheric carbon dioxide](#). *Phil. Trans. R. Soc. A*, **371**, 20120294, doi:10.1098/rsta.2012.0294.
- ²⁰ www.google.com/search?q=walker+circulation&tbm=isch&itbo=u&source=univ&sa=X&ei=bU_dUsDYBPSvsQTb2oCYDw&sqi=2&ved=0CDYQsAQ&biw=1600&bih=713
- ²¹ <http://www.cpc.ncep.noaa.gov/products/precip/CWlink/MJO/enso.shtml#discussion>
- ²² Hansen, J., M. Sato, R. Ruedy, K. Lo, D.W. Lea, and M. Medina-Elizade, 2006: [Global temperature change](#). *Proc. Natl. Acad. Sci.*, **103**, 14288-14293, doi:10.1073/pnas.0606291103.
- ²³ McGregor, S., A. Timmermann, M.H. England, O.E. Timm, A.T. Wittenberg, 2013: Inferred changes in El Niño-Southern Oscillation variance over the past six centuries. *Clim. Past* **9**, 2269-2284.
- ²⁴ Cai, W. and 13 co-authors, 2014: Increasing frequency of extreme El Niño events due to greenhouse warming. *Nature Clim. Change*, publ. on-line 19 January 2014 doi:10.1038/NCLIMATE2100